ELECTRIC DIPOLE STRENGTH BELOW THE GIANT DIPOLE RESONANCE*

J. Enders, M. Babilon, T. Hartmann, A. Heine P. von Neumann-Cosel, V.Yu. Ponomarev, N. Ryezayeva S. Volz, A. Zilges

Institut für Kernphysik, Technische Universität Darmstadt
D–64289 Darmstadt, Germany

and T. Guhr

Mathematisk Fysik, LTH, Lunds Universiteit, S-22100 Lund, Sweden

(Received November 30, 2004)

Recent experimental findings and theoretical approaches to the electric dipole (E1) strength distribution below the particle emission threshold at shell closures are revisited. Results from photon scattering experiments are discussed and compared to predictions within the quasiparticle–phonon nuclear model. An analysis of the fine structure of the E1 strength is presented. Recent studies of the E1 response of light exotic nuclei are also discussed.

PACS numbers: 23.20.Lv, 24.30.–v, 24.60.Lz, 25.20.–x

1. Introduction

The electric dipole (E1) response below the particle separation energy has been subject of many investigations. More than thirty years ago, an accumulation of E1 strength around 5–7 MeV was detected in neutron capture reactions [1] and has been dubbed "pygmy dipole resonance" (PDR) in comparison to the "giant" resonance (GDR) that dominates the E1 response and exhausts the Thomas–Reiche–Kuhn oscillator sum rule. The origin of the low-lying strength has been discussed within several models. For an overview over the various approaches we refer to [2] and Refs listed therein.

* Presented at the XXXIX Zakopane School of Physics — International Symposium "Atomic Nuclei at Extreme Values of Temperature, Spin and Isospin", Zakopane, Poland, August 31–September 5, 2004.

In recent years, it has become possible to significantly increase the sensitivity in photon scattering experiments due to the advent of new accelerators and more efficient detection systems. Additionally, new facilities studying exotic ions far from stability have revealed evidence for a "soft" E1 resonance which might be related to the number of valence neutrons. Experimental *and* theoretical analysis is needed to pin down the structure of the PDR in a consistent way, *i.e.*, to elucidate if the low-lying E1 strength is found to originate from one mechanism throughout the nuclear chart. One proposed motion underlying the PDR is an out-of-phase oscillation of the excess neutrons with respect to an $N \approx Z$ core in comparison to the GDR where all protons and neutrons oscillate out of phase. Such a mode was first suggested by Mohan *et al.* [3].

2. Experimental techniques

2.1. Real photon scattering

The resonant scattering of real photons or nuclear resonance fluorescence (NRF) is an established tool for measuring low-multipolarity excitations of bound states [4]. It allows one to determine angular momenta, excitation energies, and transition strengths. In recent years, NRF experiments have been performed with unpolarized bremsstrahlung at the continuous electron accelerators in Darmstadt (S–DALINAC [5]) and Stuttgart (Dynamitron [4]). Polarized electrons in the entrance channel have been used at the former bremsstrahlung facility in Ghent [6] and are planned for the new superconducting ELBE accelerator [7] in Rossendorf near Dresden. Laser Compton backscattering facilities in the low MeV range have become available recently. Here, full linear polarization can be achieved, and the photon spectrum is limited to a narrow region which is determined by the laser energy, the electron energy and the opening angle of the scattered radiation. Highest fluences have been achieved at the Duke high-intensity gamma source HIγS [8] through intra-cavity backscattering of a free-electron laser beam at a storage ring.

Most of the experiments described below have been performed at the S–DALINAC with unpolarized photon scattering. The bremsstrahlung is produced from electron beams with energies variable between 3 and 10 MeV that have average currents of up to 60 μA. A copper collimator cuts out the central part of the bremsstrahlung cone. Two actively shielded high-purity germanium detectors with an efficiency of 100% relative to a 3"×3" NaI(Tl) crystal at 1.33 MeV are used for the detection of the scattered photons. Recently, a third detector of the same type has been added to this setup and will be used for future experiments.

2.2. Coulomb excitation and breakup

While real photon scattering — at least up to now — is only possible on stable targets with target masses in excess of a few hundred mg, short-lived radioactive nuclei can be studied in Coulomb excitation [9] if one uses inverse kinematics [10]. To study the E1 response up to the particle threshold, intermediate-energy to relativistic beams are used. At these velocities, the emitted γ rays are forward-focused, and their energy in the laboratory frame depends on the emission angle due to the Doppler effect. Recent examples of E2 excitations are presented in these proceedings. For excitations above the particle threshold, neutrons are emitted which are also forward-focused and can be measured near 0° with coverage of the full solid angle in the center-of-mass system.

3. Quadrupole-octupole two-phonon E1 excitations

Two-phonon excitations are a well-known phenomenon in vibrational nuclei [11]. If one couples an elementary quadrupole vibration to an octupole vibrational mode, one ends up with a quintuplet of states with $J^\pi = 1^- \ldots 5^-$; its 1^- member can be excited from the ground state by an E1 transition. These two-phonon 1^- states can be used to study anharmonicities in the coupling of two different phonons and the strength of its coupling to the isovector GDR. One can investigate their isospin structure and identify the structure of the two-phonon wavefunction by measuring the decay pattern. The latter has been pioneered by a group from Cologne in $(p, p'\gamma)$ reactions [12].

Candidates for such two-phonon states have been found at the shell closures $Z = 20$ [13, 14], $N = 28$ [15], $N = 50$ [16], $Z = 50$ [17, 18] and $N = 82$ [4]. Further evidence was found in many open-shell nuclei [19]. In rotational nuclei, the first 1^- state becomes the head of the octupole vibrational band with $K^\pi = 0^-$; results of a survey have been compiled, *e.g.*, by Fransen and co-workers [20].

4. 'Pygmy' dipole resonance

4.1. Coulomb excitation and breakup of light exotic oxygen isotopes

Pioneering experiments at the Cyclotron Laboratory at Michigan State University and at the ALADIN/LAND setup at the GSI have studied the Coulomb excitation and Coulomb breakup, respectively, of stable and neutron-rich oxygen isotopes. Tryggestad and co-workers [21] have studied the E1 response of ^{20}O in comparison to ^{18}O with Coulomb excitation up to the particle threshold. They found an increase in the detected E1 strength in the

more neutron-rich isotope. Leistenschneider *et al.* [22] measured the photoneutron yield from the particle threshold up to about 30 MeV in $^{17-22}$O. In the interval up to 15 MeV — where the GDR in the "core" nucleus ^{16}O sets in — about 50–70% of the cluster sum rule and 5–10% of the E1 strength is spread out over a wider energy interval in the neutron-rich systems compared to the ^{16}O "core".

4.2. The calcium isotopes

The E1 strength distribution in the two doubly magic nuclei ^{40,48}Ca has been studied in photon scattering at the S–DALINAC up to an energy of 10 MeV by Hartmann *et al.* [13]. The data demonstrate that the summed low-lying strength in the neutron-rich ($N/Z = 1.4$) ^{48}Ca is more than a factor of 10 larger than in the $N = Z$ nucleus ^{40}Ca. Qualitatively, this is what is expected from a "neutron-skin" vibration, but predictions within density functional theory [23] cannot quantitatively describe the measured values. Earlier attempts to extract the E1 strength from inelastic heavy-ion scattering [24] suffer from a model dependence and disagree with the high-resolution photon scattering data.

Recent experiments [25] on ^{44}Ca detected an E1 strength up to 10 MeV that is even larger than in ^{48}Ca. Attempts to reproduce this finding and the ^{40,48}Ca data within the extended theory of finite Fermi systems [26] have been performed successfully and qualitatively describe the data [25].

4.3. The $N = 50$ isotones

At the $N = 50$ shell closure, unpublished data from the Ghent group exist for ^{92}Mo as well as data on ^{88}Sr measured at the S–DALINAC [27]. Recently, the new NRF facility at Rossendorf has started to map the E1 strength in nuclei in this region.

4.4. The tin isotopes

A study of the Sn isotopes ^{116,124}Sn has been performed at the Ghent linac nearly a decade ago [6]. Govaert and co-workers have found appreciable E1 strength below the neutron separation energy in both nuclei, with the value for ^{124}Sn being significantly larger than the one observed for the less neutron-rich isotope with mass 116. This finding could not be reproduced by quasiparticle–phonon model (QPM) calculations which expect the pygmy E1 strength to be maximal at mass 120, whereas for ^{116,124}Sn comparable summed E1 strengths are expected. However, in the QPM calculations the mean-field parameters are not varied between the different isotopes, and the interactions are chosen to reproduce collective low-lying modes. To shed

further light on this discrepancy between theory and experiment, a photon scattering experiment on the most proton-rich stable isotope ^{112}Sn has been performed at the S–DALINAC. Data analysis is in progress [28].

4.5. The $N = 82$ isotones

The $N = 82$ isotones ^{138}Ba, ^{140}Ce, and ^{144}Sm have been subject of recent studies at the S-DALINAC and have been published by Zilges *et al.* [29]. In the more neutron-rich nucleus ^{138}Ba, more E1 strength was found than in the other isotones. In the recently measured ^{142}Nd [30], the detected E1 strength is about as low as in ^{140}Ce and ^{144}Sm. The observed variation of the total E1 strength is not reproduced by the QPM which expects constant summed E1 strengths in all nuclei. Figure 1 summarizes the experimental data as well as the QPM predictions for the four isotones. The lowest E1 excitation populates the two-phonon quadrupole–octupole 1^- state discussed in the preceding section. From laser Compton backscattering it is known that strong dipole excitations observed in this energy region exhibit electric character [31].

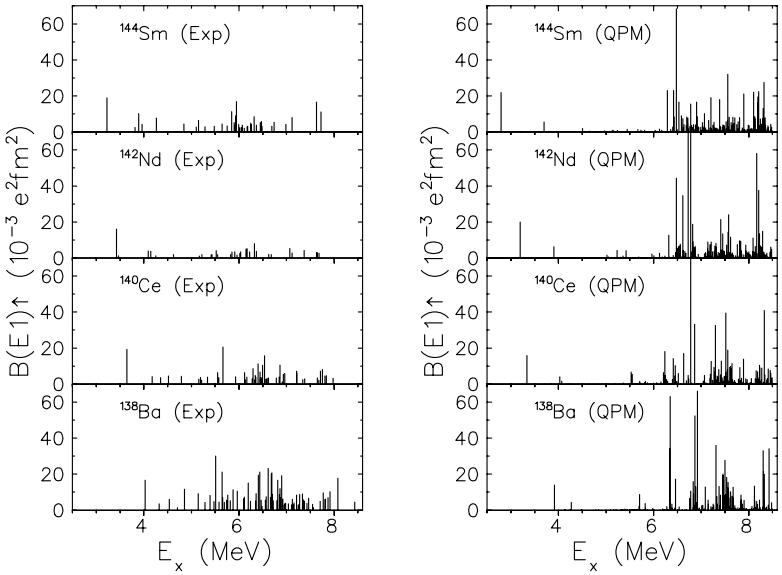

Fig. 1. Left: Experimental E1 strength distributions up to 8.5 MeV in ^{138}Ba, ^{140}Ce, ^{142}Nd, and ^{144}Sm from photon scattering [29, 30]. Right: Electric dipole strength distributions as calculated from the QPM. While the overall fragmentation process due to coupling to complex configurations is adequately described by the QPM, the model predictions show only little variation of the summed E1 strength in contrast to experiment.

It is suggestive to assume a dependence of the summed E1 strength on macroscopic quantities, such as the difference between proton and neutron radii, $|r_n - r_p|$. Measurements from antiproton capture and annihilation reactions [32] indicate that $|r_n - r_p|$ is minimal in ^{142}Nd for even-A nuclei with $N = 82$, whereas for the proton-deficient ^{138}Ba indications for a neutron-rich periphery are observed. A photon scattering experiment on ^{136}Xe — where the neutron excess is even larger — could help clarify this situation. The experimental feasibility of NRF experiments with high-pressure Xe gas targets has been demonstrated recently at the Stuttgart Dynamitron [33].

4.6. The lead isotopes

A concentration of low-lying E1 strength in ^{206,207,208}Pb is known from early NRF experiments, see, *e.g.*, the survey by Chapuran *et al.* [34]. Recently, a precise data set for these nuclei has been obtained which extended the systematics for the first time to the neutron-deficient ^{204}Pb [2,35] up to 6.7 MeV. A strong fragmentation of the low-lying E1 strength is observed with the opening of the $N = 126$ neutron shell which is well reproduced by the quasiparticle–phonon model.

It is instructive to compare the measured E1 strength distribution with an extrapolation of the isovector GDR to study if the low-lying strength might simply be a part of the giant resonance. Figure 2(a) shows this comparison for ^{204,206,208}Pb. The hatched histograms show the experimental data extracted by binning the measured E1 strength. The solid curve shows an extrapolation of the GDR assuming a constant width. From neutron capture reactions and other measurements of gamma strength functions close to the particle threshold it is known that such an extrapolation of the GDR Lorentzian overestimates the actual E1 strength in nuclei at or near closed shells. Kopecky and Uhl [36] thus suggested to use a Lorentzian with an energy-dependent width which is shown as dotted line in Fig. 2(a). A very similar result [dashed line in Fig. 2(a)] is obtained by introducing a dipole-quadrupole interaction term as suggested by Mughabghab and Dunford [37] that effectively includes dynamical deformations. In any case, a realistic extrapolation of the GDR fails to account for the detected E1 strength and its concentration between 5 and 6 MeV.

The doubly magic nucleus ^{208}Pb has been studied using an even higher endpoint energy of 9.0 MeV by Ryezayeva *et al.* [38], and a considerable number of states was detected even beyond the neutron separation energy. The E1 excitation strength was extracted from the photon scattering data using known neutron decay widths. It is well reproduced within the QPM. Due to the good agreement between theory and experiment, one may ask about the structure that the model predicts for the low-lying states. Analyzing

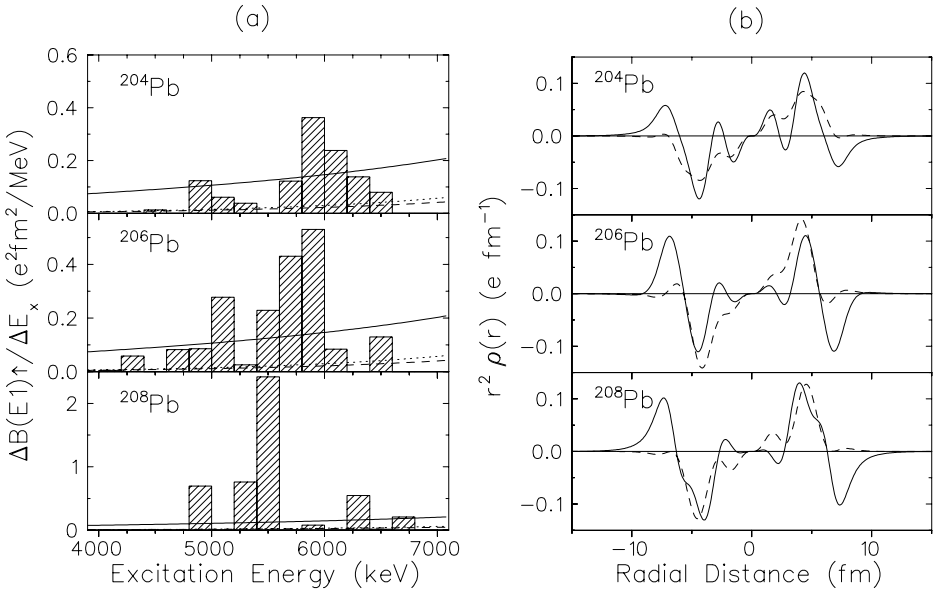

Fig. 2. (a) Comparison of experimentally determined E1 strength distributions (histograms) with extrapolations of the giant dipole resonance (GDR). The solid curves display the extrapolation with a constant width of the GDR, the dotted curves assume an energy-dependent width, and the dashed curve includes dynamical deformations according to Mughabghab and Dunford [37]. (b) Calculated average charge transition density distributions for ^{204,206,208}Pb from the quasiparticle–phonon model for energies up to 8 MeV. The solid curves display the neutron densities, the proton densities are shown by the dashed curve. In all three nuclei, an out-of-phase oscillation of the outer neutrons with respect to a neutron–proton fluid is visible.

the average charge transition density distributions for states below 8 MeV, one finds a distinct pattern in which the outer neutrons oscillate against a combination of protons and neutrons. This is displayed for ^{204,206,208}Pb in Fig. 2(b) where the solid lines depict the neutron and the dashed lines proton densities. In addition, the average current distribution shows the presence of a toroidal mode in the same energy region. While the "neutron skin" vibration seen in the transition densities dominates the B(E1) strength, the toroidal mode can be prepared out, *e.g.*, in backward-angle electron scattering. Such experiments with detailed form-factor measurements are planned at the S-DALINAC in the future.

5. Statistical analysis of the fine structure of the pygmy resonance

As has been shown in the previous section, detailed information about the fine structure of the pygmy E1 mode has been obtained from NRF experiments. The statistical properties of the fine structure contain information about the underlying dynamics: Whereas for low-spin states at high excitation energies (around the particle separation threshold) the level spacing shows strong correlations and is in agreement with the expectations of random matrix theory [39], low-lying modes in deformed nuclei have been found to exhibit more regular features with random level spacings [40]. A particularly interesting example in this respect is the collective scissors mode where a random nearest-neighbor spacing distribution (NND) has been found [41].

184 states with $J^\pi = 1^-$ in the four $N = 82$ isotones ^{138}Ba, ^{140}Ce, ^{142}Nd, and ^{144}Sm have been combined to form a common data ensemble after unfolding the energy dependencies of the level density for the different nuclei individually. Figure 3 displays that intermediate behavior between the extremal cases of correlated (Wigner, dash-dotted) and random (Poisson, dashed) distributions is found [42]. For the interpretation of this result it is important to point out that a large fraction of the expected states is not detected experimentally due to a finite detection threshold. Cutting out states based on their excitation strength, *i.e.*, randomly with respect to their excitation energy, leads gradually to a random NND even if the full level sequence was correlated, as lately discussed in [43,44]. The experimental finding of an intermediate NND can be explained only if one assumes that the level spacings distribution of the underlying complete spectrum exhibits strong spectral correlations. This can be ascribed to the rather high level density and is rather independent from the underlying non-collective or collective structure of the excitation mode.

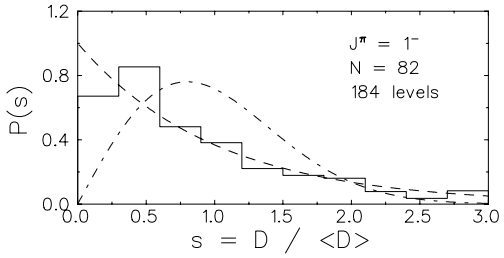

Fig. 3. Nearest-neighbor spacing distribution for an ensemble of 184 $J^\pi = 1^-$ states in the $N = 82$ isotones (solid histogram). For comparison, the random Poissonian distribution (dashed) and the correlated Wigner distribution (dash-dotted) are shown.

6. Astrophysical impact

The dipole strength distribution at the particle separation energies might affect reaction rates in astrophysical scenarios where photodisintegration reactions are important, *i.e.*, in hot stars and stellar explosions. In recent years, pioneering experiments have been carried out at the S-DALINAC to study photoactivation of heavy nuclei in order to elucidate their production mechanisms in p- and s-process sites [45,46]. Measuring the activation yields at different endpoint energies of the bremsstrahlung yields a determination of the reaction rate that is largely independent from details of the threshold behavior of the photoneutron cross sections.

While the activation experiments using bremsstrahlung can probe cold nuclei only, nuclei in the stellar environment will be thermally excited. Thus, the extracted data can only be compared with the predictions from statistical model calculations for this single channel, but they provide for a test of the input data for astrophysical network calculations.

7. Conclusion

An overview over recent experiments studying electric dipole strength excited by nuclear resonance fluorescence and Coulomb excitation from the ground state in semi and doubly magic nuclei has been presented. One finds that in neutron-rich systems the low-lying E1 strength is enhanced. Microscopic quasiparticle–phonon model calculations facilitate a good overall description of the experimental data in heavy nuclei. The general agreement between theory and experiment allows one to extract nuclear structure properties from the model which also points to an out-of-phase oscillation of the outer neutrons with respect to a joint motion of protons and neutrons in the nuclear interior. The calculations furthermore indicate the presence of a toroidal, transversal E1 mode centered at about $1\hbar\omega$.

The statistical properties of the fine structure of the pygmy resonance in the $N = 82$ isotones have been analyzed, and in light of the large number of missing levels, indications for strong correlations have been found. The level density in the investigated energy region at the shell closure is already sufficiently high to infer spectral correlations. The knowledge about the level spacing distribution might in turn be used to extract level densities in the PDR region by means of a fluctuation analysis [47, 48].

It has been pointed out that the knowledge about the E1 strength function close to the threshold has important implications on astrophysical reaction rates in nuclei where photodissociation reactions are important. The cross section starting from the ground state measured in NRF and photoactivation represents an important test of nuclear structure and reaction models used in nucleosynthesis network calculations.

Several open questions about the origin of the low-lying E1 strength remain, *e.g.* about its isospin character. This will be studied in alpha scattering reactions at KVI Groningen in the near future. A detailed analysis of the E1 form factors as well as an attempt to prepare out components of the toroidal mode in the transverse response will be undertaken in electron scattering [49]. The available data on low-energy E1 strength in nuclei far from stability are very scarce, and more systematic studies are needed. One example for such an experiment is the proposed investigation of E1 strength below the particle threshold in ^{68}Zn to be measured with the RISING setup at the GSI.

It is a pleasure to thank P. Mohr, A. Richter, and J. Wambach for enlightening discussions. This work profited also from a long-standing research collaboration with the groups of P. von Brentano and U. Kneissl, and the nuclear structure group at the research center Rossendorf. JE thanks the organizers of the Zakopane school for creating a very stimulating atmosphere and putting together an interesting program. This work was supported by the Deutsche Forschungsgemeinschaft through Sonderforschungsbereich 634. TG acknowledges funding from the Det Svenska Vetenskapsraadet.

REFERENCES

[1] G.A. Bartholomew *et al.*, *Adv. Nucl. Phys.* **7**, 229 (1972).

[2] J. Enders *et al.*, *Nucl. Phys.* **A724**, 243 (2003).

[3] R. Mohan, M. Danos, L.C. Biedenharn, *Phys. Rev.* **C3**, 1740 (1971).

[4] U. Kneissl, H.H. Pitz, A. Zilges, *Prog. Part. Nucl. Phys.* **37**, 349 (1996).

[5] P. Mohr *et al.*, *Nucl. Instrum. Methods in Phys. Res.* **A423**, 480 (1999).

[6] K. Govaert *et al. Phys. Rev.* **C57**, 2229 (1998).

[7] M. Erhard *et al.*, Proceedings of the Internatl. Workshop XXXII on Gross Properties of Nuclei and Nuclear Exciations, Hirschegg/Austria, 125 (2004).

[8] N. Pietralla *et al.*, *Nucl. Instrum. Methods in Phys. Res.* **A483**, 556 (2002).

[9] K. Alder, A. Winther, *Electromagnetic Excitation*, North–Holland Publishing, Amsterdam 1975.

[10] T. Glasmacher, *Annu. Rev. Nucl. Part. Sci.* **48**, 1 (1998).

[11] A. Bohr, B.R. Mottelson, *Nuclear Structure, Vol. II*, Benjamin, Reading/MA 1975.

[12] M. Wilhelm *et al.*, *Phys. Rev.* **C54**, R449 (1996).

[13] T. Hartmann *et al.*, *Phys. Rev. Lett.* **85**, 274 (2000); *Phys. Rev. Lett.* **86**, 4981 (2001) (Erratum).

[14] T. Hartmann *et al.*, *Phys. Rev.* **C65**, 034301 (2002).

[15] J. Enders *et al.*, *Nucl. Phys.* **A636**, 139 (1998).
[16] N. Pietralla *et al.*, *Phys. Rev.* **C65**, 047305 (2002).
[17] J. Bryssinck *et al.*, *Phys. Rev.* **C59**, 1930 (1999).
[18] I. Pysmenetska, diploma thesis, Kharkiv Karazin University (2004).
[19] M. Babilon *et al.*, *Phys. Rev.* **C65**, 037303 (2002).
[20] C. Fransen *et al.*, *Phys. Rev.* **C57**, 129 (1998).
[21] E. Tryggestad *et al.*, *Phys. Lett.* **B541**, 52 (2002).
[22] A. Leistenschneider *et al.*, *Phys. Rev. Lett.* **86**, 5442 (2001).
[23] J. Chambers *et al.*, *Phys. Rev.* **C50**, R2671 (1994).
[24] S. Ottini-Hustache *et al.*, *Phys. Rev.* **C59**, 3429 (1999).
[25] T. Hartmann *et al.*, *Phys. Rev. Lett.*, **93**, 192501 (2004).
[26] S. Kamerdzhiev, J. Speth, G. Tertychny, *Phys. Rep.* **393**, 1 (2004).
[27] L. Käubler *et al.*, *Phys. Rev.* **C70**, 064307 (2004).
[28] I. Poltoratska, diploma thesis, Kharkiv Karazin University, (2005).
[29] A. Zilges *et al.*, *Phys. Lett.* **B542**, 43 (2002).
[30] S. Volz, Dissertation, TU Darmstadt, in preparation.
[31] N. Pietralla *et al.*, *Phys. Rev. Lett.* **88**, 012502 (2002).
[32] P. Lubinski *et al.*, *Phys. Rev.* **C57**, 2962 (1998).
[33] H. von Garrel, Dissertation, Universität Stuttgart (2004).
[34] T. Chapuran, R. Vodhanel, M.K. Brussel, *Phys. Rev.* **C22**, 1420 (1980).
[35] J. Enders *et al.*, *Phys. Lett.* **B486**, 279 (2000).
[36] J. Kopecky, M. Uhl, *Phys. Rev.* **C41**, 1941 (1990).
[37] S.F. Mughabghab, C.L. Dunford, *Phys. Lett.* **B487**, 155 (2000).
[38] N. Ryezayeva *et al.*, *Phys. Rev. Lett.* **89**, 272502 (2002).
[39] R.U. Haq, A. Pandey, O. Bohigas, *Phys. Rev. Lett.* **48**, 1086 (1982).
[40] J.F. Shriner Jr., G.E. Mitchell, T. von Egidy, *Z. Phys.* **A338**, 309 (1991).
[41] J. Enders *et al.*, *Phys. Lett.* **B486**, 273 (2000).
[42] J. Enders *et al.*, *Nucl. Phys.* **A741**, 3 (2004).
[43] U. Agvaanluvsan *et al.*, *Nucl. Instrum. Methods in Phys. Res.* **A498**, 459 (2003).
[44] O. Bohias, M.P. Pato, *Phys. Lett.* **B595**, 171 (2004).
[45] P. Mohr *et al.*, *Phys. Lett.* **B488**, 127 (2000).
[46] K. Sonnabend *et al.*, *Phys. Rev.* **C70**, 035802 (2004).
[47] P.G. Hansen, B. Jonson, A. Richter, *Nucl. Phys.* **A518**, 13 (1990).
[48] J. Enders *et al.*, *Phys. Rev. Lett.* **79**, 2010 (1997).
[49] N. Ryezayeva *et al.*, *Nucl. Phys.* **A**, submitted.